



# A fractal model for the sea state bias in radar altimetry

D. E. Bar, Y. Agnon

## ► To cite this version:

D. E. Bar, Y. Agnon. A fractal model for the sea state bias in radar altimetry. *Nonlinear Processes in Geophysics*, 1997, 4 (4), pp.213-222. hal-00301865

**HAL Id: hal-00301865**

**<https://hal.science/hal-00301865>**

Submitted on 1 Jan 1997

**HAL** is a multi-disciplinary open access archive for the deposit and dissemination of scientific research documents, whether they are published or not. The documents may come from teaching and research institutions in France or abroad, or from public or private research centers.

L'archive ouverte pluridisciplinaire **HAL**, est destinée au dépôt et à la diffusion de documents scientifiques de niveau recherche, publiés ou non, émanant des établissements d'enseignement et de recherche français ou étrangers, des laboratoires publics ou privés.

# A fractal model for the sea state bias in radar altimetry

D. E. Bar and Y. Agnon

Department of Mathematics, Technion, Haifa 32000, Israel  
Civil Engineering, Technion, Haifa 32000, Israel

Received: 29 April 1997 – Accepted: 25 May 1998

**Abstract.** The Kirchhoff approximation is used to determine the sea state bias in radar altimetry. A weakly nonlinear model of the sea waves is used to derive the joint moments of two different points separated by a distance  $\vec{R}$ ; the bias moment is formulated, and found for power law spectra. The method provides a consistent analysis of the sea state bias and avoids the need to truncate the high frequency tail of power-law wave spectra. The model exhibits dependence of the “electromagnetic bias” on the radar frequency, an effect observed in field experiments.

## 1 Introduction

Radar altimetry is a very useful tool for observing the dynamic surface height and for inferring oceanic circulation and related phenomena. The utility of altimetric observations is limited by the accuracy of the measurement. Perhaps the least success has been achieved in removing the sea state (or electromagnetic) bias.

This bias is due to a shift in the mean radar reflecting surface relative to the mean sea surface. It results from the non-Gaussianity of the sea surface, which is due to the nonlinearity of the surface waves.

Quite a few studies of the sea state bias have been carried out in recent years. Most of the efforts to model the radar reflection were based on the specular point reflection model (Barrick and Lipa, 1985; Srokosz, 1986, 1987). This model encounters difficulties (lack of convergence) when applied to typical wave spectra which have power-law high frequency tails (Agnon and Stiassnie, 1991; Glazman, 1990; Glazman and Weichman, 1989; Phillips, 1985; Stiassnie et al., 1991). Such spectra can be characterized as the spectra of fractal surfaces (Stiassnie, 1988), if the range of scales of interest lies within the spectral range for which self-affinity holds (Stiassnie

et al., 1991). A common approach to this difficulty was to introduce a high wave number cutoff to the sea wave spectrum. It has been argued that this cutoff could be related to the radar frequency, and thus the (observed) variation of the sea state bias with the radar frequency could be accounted for.

The approach taken in the present study, is to use a more general reflection model for the radar signal. This is the Kirchhoff approximation, which had been applied to determining the radar cross section of the sea surface (Agnon and Stiassnie, 1991; Berry and Blackwell, 1981; Yordanov and Stoyanov, 1989). It has the advantage that it can describe the reflection from a surface with a power law spectrum. In the present model it is not necessary to introduce a cutoff just to get finite results. We do however introduce a cutoff in order to describe more accurately the sea wave spectrum. This cutoff is based on the hydrodynamics and is not related to the radar wavelength.

Theoretical estimates of the sea state bias range from 1% up to 8% of the significant wave height (SWH) (Born and Richards, 1982; Glazman et al., 1996, 1994; Glazman and Srokosz, 1991). In field experiments of Walsh et al. (1989, 1991), an approximate relation was found to hold between the radar frequency and the sea state bias

$$\frac{\text{sea state bias}}{\text{SWH}} = (3.0 - 0.0617F)(1 \pm 0.5) \% \quad (1)$$

where  $F$  is the radar frequency in GHz (in the experiments  $F = 5.3, 10, 13.6, 36$ ). Thus, the sea state bias is smaller for shorter radar waves. The specular point reflection model does not account for this dependence.

A notable exception to the geometric optics approach is the work of Rodriguez et al. (1992). They used direct numerical simulations of radar backscatter in a Monte Carlo approach. Their work requires separation of the spectrum into long and short scale waves. Due to its computational intensiveness, they were limited to studying one dimensional surface profiles.

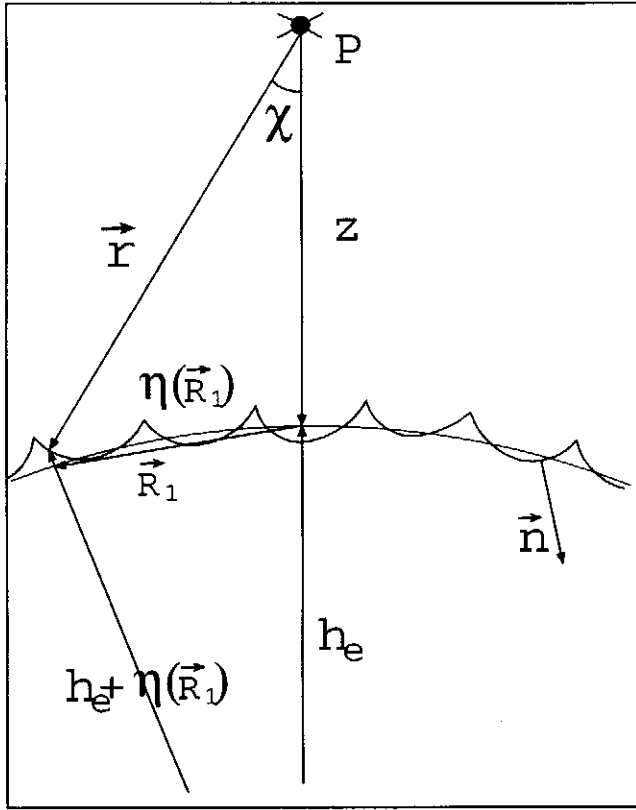


Fig. 1. Geometry of diffracted echos from the ocean surface. The satellite is at  $P$ , at a height  $z$  above the mean sea level. The pulse is reflected from the point at  $\vec{r}$  relative to the satellite, at an elevation  $\eta(\vec{R}_1)$  above the mean sea level.  $\vec{R}_1$  is measured from the zenith point.  $\vec{r}$  forms an angle  $\chi$  with the vertical.  $h_e$  is the radius of earth and  $\vec{n}$  is the normal to the sea surface pointing inwards.

In the present work we introduce a model which is capable of accounting for the frequency dependence of the reflected signal, while maintaining relative simplicity.

The mathematical problem is formulated in the next section. Section 3 discusses the statistical properties of the ocean waves. The joint moments and the joint distribution function will be presented, where special consideration will be given to the BIAS moment and its characteristics. In Sections 4 and 5, the intensity integral is solved and a general form for the sea state bias will be given. Finally, numerical results and conclusions are given in Sections 6 and 7.

## 2 Formulation of the diffracted radar pulse by Kirchoff approximation

The geometry of the problem is shown in Fig. 1. The satellite, which is located at point  $P$  at the height  $z$  above the average sea level, sends a radar pulse  $\Phi_0 = \Phi_0(\vec{r}, t, \chi)$ , where  $\vec{r}$  is the vector from the satellite point  $P$ ,  $t$  is the time and  $\chi$  is the angle from the zenith point.

We assume a quasi-monochromatic pulse:

$$\Phi_0 = \frac{f_0(t - r/c)}{r} g(\chi) \quad (2)$$

$$f_0(T) = e^{i\omega_\lambda T} a(T) \quad (3)$$

$$a(T) = a_0 \exp\left\{-\frac{c^2 T^2}{\sigma^2}\right\} \quad (4)$$

In general, the pulse shape  $g(\chi)$  depends on the pulse length,  $\sigma$ , the time interval of reading the return pulse and the satellite type. As an example, we can assume

$$g(\chi) = \begin{cases} 1 & \text{when } |\chi| \leq \chi_{max} \\ 0 & \text{when } |\chi| > \chi_{max} \end{cases} \quad (5)$$

$$\chi_{max} \approx 0.3^\circ = \pi/600 \text{ radians} \ll 1. \quad (6)$$

The frequency  $\omega_\lambda = ck_\lambda = 2\pi c/\lambda$ , where:  $c$  the speed of light;  $k_\lambda$  the wave number;  $\lambda$  wave length;  $a(T)$  is a Gaussian envelope. To make sure that the pulse is quasi-monochromatic we will assume

$$\lambda \ll \sigma. \quad (7)$$

For SEASAT  $\lambda = 0.03m$ ,  $\sigma = 3m$ . This value of  $\lambda$  is also inside the range of wavelengths used in TOPEX.

For electromagnetic waves  $c$  is the speed of light, and the sea surface will appear frozen to the radar pulse. Therefore, we assume that the height of the sea surface,  $\eta(\vec{R}_1)$ , is fixed during the time interval of the measurement.  $\vec{R}_1$  is the average surface vector measured from the zenith point to the satellite.

$r$  can be related to  $\eta(\vec{R}_1)$  and  $R_1$ , using  $z$  and  $h_e$  (the radius of Earth) by a simple geometric consideration. Using the cosine theorem (see Fig. 1) we get the algebraic equations:

$$(h_e + \eta(\vec{R}_1))^2 = (h_e + z)^2 + r^2 - 2r(h_e + z) \cos \chi \quad (8)$$

$$\eta^2(\vec{R}_1) + R_1^2 = z^2 + r^2 - 2rz \cos \chi \quad (9)$$

where we assume:  $|\chi| < \chi_{max}$ ,  $R_1/z = O(\chi_{max})$ ,  $\eta(\vec{R}_1)/z = O(\chi_{max}^2)$ . From those equations we get an estimate for  $r$ :

$$\frac{r}{z} = 1 - \frac{\eta(\vec{R}_1)}{z} + \frac{R_1^2}{2z'^2} + O(\chi_{max}^4). \quad (10)$$

Where  $z' = h_e z / (h_e + z)$  is the reduced height due to Earth's curvature. Typically  $z \approx 800km$ , Earth radius  $h_e = 6370km$  and the reduced height  $z' \approx 710km$ .

Our purpose is to study the sea state bias by better understanding the time dependence of the nadir reflection of a quasi-monochromatic radar pulse  $\Psi$  from a fractal (i.e. with a power law spectrum) sea surface. Specifically, we are interested in the effect of the ocean waves nonlinearity on the intensity of the reflected pulse:

$$I = \langle |\Psi(\tau)|^2 \rangle \quad (11)$$

as a function of the time  $\tau$  measured from the time  $t = 2z/c$  at which the mid-pulse will return from the

zenith point.  $\langle f \rangle$  is the average of a functional  $f$  over the probability space. In our case we deal with the sea waves probability which will be given later.

Using Kirchhoff's approximation (e.g., Berry, 1972) we have the reflected pulse as a superposition of waves from secondary sources on the sea surface:

$$\Psi(\tau) = \frac{1}{2\pi c} \iint d\vec{R}_1 \frac{1}{r^2} f'_0 \left( \tau + \frac{2\eta(\vec{R}_1)}{c} - \frac{R_1^2}{cz'} \right) \frac{d\vec{r}}{d\vec{n}} \quad (12)$$

For Gaussian distribution of the sea surface height this function is anti-symmetric about the mid-point,  $\tau = 0$  (Berry and Blackwell, 1981). The sea state bias is a small offset, due to the nonlinearity (or non Gaussian nature) of the distribution function of the sea surface height. This nonlinearity appears as pointed crests and flattened troughs. Therefore, we expect that the derivative of the intensity will be smaller for  $\tau < 0$  than the one for  $\tau > 0$  (when more energy will be reflected). This will be seen from the calculation (and was shown by previous models). Intuitively, the pointed crests are a rougher surface than the flattened troughs, hence the crests produce smaller reflection.

We note that

$$\frac{1}{r^2} = \frac{1}{z^2} (1 + O(\chi_{max}^2)) \quad (13)$$

Also, from the asymptotic expansion for the sea surface height, in the wave steepness  $\epsilon$ :

$$\frac{d\vec{r}}{d\vec{n}} = 1 + O(\epsilon^2) \quad (14)$$

The value 1 is simply the cosine of the incidence angle (which is  $\pi/2$ ). It should be modified for other radar applications, in which the incidence is not along the normal to the surface.

Since the pulse is quasi-monochromatic, we can write the derivative (using  $T = O(\tau)$ ,  $k_\lambda = \omega_\lambda/c$ ) as:

$$f'_0(T) = i\omega_\lambda f_0(T) (1 + O(c\tau/k_\lambda\sigma^2)) \quad (15)$$

following Berry and Blackwell (1981). We see that the pulse envelope term  $c\tau/k_\lambda\sigma^2$  will be smaller than  $O(\epsilon^2)$ .

When  $\chi_{max} \lesssim \epsilon$  (which is true for any realistic wavy sea, since  $\chi_{max} \approx 5 \cdot 10^{-3}$  (Eq. 6) and the wave steepness is typically  $0.01 < \epsilon$ ), the equation for the return pulse is given by:

$$\Psi(\tau) = \frac{ik_\lambda}{2\pi z^2} \iint f_0(T_1) d\vec{R}_1 \quad (16)$$

$$T_i = \tau + 2\eta(\vec{R}_i)/c - R_i^2/cz' \quad (17)$$

and the intensity integral is given by:

$$I = \left( \frac{k_\lambda}{2\pi z^2} \right)^2 \iint d\vec{R}_1 \iint d\vec{R}_2 \left\langle a(T_1)a(T_2)e^{-2ik_\lambda(\eta(\vec{R}_1)-\eta(\vec{R}_2))} \right\rangle e^{ik_\lambda(R_1^2-R_2^2)/z} \quad (18)$$

To calculate this integral the appropriate probability function needs to be taken. In our formulation, it will be the joint probability function of the height and its increment at two points,  $\vec{R}_1$  and  $\vec{R}_2$ , on the average sea surface. This is in contrast to specular point reflection models in which joint moments of the height and slope at a single point appear. It will be shown that the present formulation gives convergent results for power law spectra, for which specular point reflection gave divergent values.

### 3 Sea surface statistics

In order to calculate the joint moments and thereafter the joint distribution functions, we consider a weakly nonlinear model of the sea surface's height:

$$\eta(\vec{x}, t) = \epsilon\eta_1 + \epsilon^2\eta_2 + O(\epsilon^3) \quad (19)$$

$\epsilon \ll 1$  represents the order of the waves' slope. For the deep water limit,  $\eta_1$  and  $\eta_2$  are found by using the theory of Longuet-Higgins (1963):

$$\eta_1 = \sum_{i=1}^n a_i \cos \phi_i \quad (20)$$

$$\eta_2 = \frac{1}{2} \sum_{i,j=1}^n a_i a_j (C_{ij} \cos \phi_i \cos \phi_j + S_{ij} \sin \phi_i \sin \phi_j) \quad (21)$$

$$\phi_i = \vec{k}_i \cdot \vec{x} - \omega_i t + \theta_i \quad (22)$$

$$\omega_i^2 = gk_i \quad (23)$$

$$C_{ij} = \frac{(B_{ij}^- + B_{ij}^+ - \vec{k}_i \cdot \vec{k}_j + (k_i + k_j)\sqrt{k_i k_j})}{\sqrt{k_i k_j}} \quad (24)$$

$$S_{ij} = (B_{ij}^- - B_{ij}^+ - k_i k_j) / \sqrt{k_i k_j} \quad (25)$$

$$B_{ij}^\pm = \frac{(\sqrt{k_i} \pm \sqrt{k_j})^2 (\vec{k}_i \cdot \vec{k}_j \mp k_i k_j)}{((\sqrt{k_i} \pm \sqrt{k_j})^2 - |\vec{k}_i \pm \vec{k}_j|)} \quad (26)$$

where:

$\theta_i$  is a probability variable evenly distributed over  $[-\pi, \pi]$ ,

$a_i$  is a Rayleigh distributed probability variable,

$\vec{k}$  is the wave number and  $k = |\vec{k}|$ ,

$w$  is the wave frequency and

$g$  is gravity.

As  $k_j \rightarrow k_i$ ,  $B_{ii}^\pm$  both vanish, which leads to  $C_{22} + S_{22} = 0$  (for example).

### 3.1 Joint moments

We start by calculating the joint moments of the sea surface elevation at two points. Since the surface is homogeneous, the joint moments will be functions of the difference in position,  $\vec{R}$ :

$$\mu_{ij} \equiv \mu_{ij}(\vec{R}) = \left\langle \eta(\vec{x})^i \eta(\vec{x} + \vec{R})^j \right\rangle. \quad (27)$$

At the limits  $n \rightarrow \infty$  and  $\frac{1}{2}\langle a_i^2 \rangle \rightarrow 0$ , we may write:

$$\epsilon^2 \sum_{\vec{k}_i \in d\vec{k}} \frac{1}{2} \langle a_i^2 \rangle = F(\vec{k}) d\vec{k} + O(|d\vec{k}|^2). \quad (28)$$

$F(\vec{k})$  is the waves energy spectrum, where  $\vec{k}$  is the wave vector. Thus we can describe the joint moments by integrals:

$$\mu_{10} = \langle \eta(\vec{x}) \rangle = \iint F(\vec{k})(C_{11} + S_{11})d\vec{k} = 0 \quad (29)$$

$$\begin{aligned} \mu_{11} &= \langle \eta(\vec{x})\eta(\vec{x} + \vec{R}) \rangle \\ &= \iint F(\vec{k}) \cos(\vec{k} \cdot \vec{R})d\vec{k} + O(\epsilon^4) \end{aligned} \quad (30)$$

$$\begin{aligned} \mu_{21} &= \langle \eta(\vec{x})^2 \eta(\vec{x} + \vec{R}) \rangle = \frac{1}{2} \iint d\vec{k}_1 \iint F(\vec{k}_1)F(\vec{k}_2) \\ &\times [(C_{12} - S_{12}) \cos((\vec{k}_1 + \vec{k}_2) \cdot \vec{R}) \\ &+ (C_{12} + S_{12}) \cos((\vec{k}_1 - \vec{k}_2) \cdot \vec{R}) \\ &+ 4C_{12} \cos(\vec{k}_1 \cdot \vec{R})] d\vec{k}_2 + O(\epsilon^6) \end{aligned} \quad (31)$$

and so on. The integration is on the surface  $\vec{k}$ ,  $d\vec{k} = k d\theta dk$ . Some of these moments are well known (Longuet-Higgins, 1963; Srokosz, 1986):

1. The average sea surface height is zero:  $\mu_{10} = 0$ .
2. The significant wave height is  $H_{1/3} = 4H$ . Where

$$H^2 = \mu_{20} = \iint F(\vec{k})d\vec{k} \quad (32)$$

3. The skewness, which is a positive number,  $\mu_{30}$ :

$$\mu_{30} = 3 \iint d\vec{k}_1 \iint F(\vec{k}_1)F(\vec{k}_2)C_{12}d\vec{k}_2 \quad (33)$$

The homogeneity of the sea surface will result in symmetry in the moments  $\mu_{ij} = \mu_{ji}$  and symmetry in  $\vec{R}$ ,  $\mu_{ij}(\vec{R}) = \mu_{ij}(-\vec{R})$ .

In contrast with the mean square slope which diverges at the short scales ( $k \rightarrow \infty$ ) for a power-law spectrum (Glazman, 1994; Phillips, 1985; Stiassnie et al., 1991)

$$F(\vec{k}) = Ak^{-\alpha} \quad (34)$$

with  $\alpha < 4$ , there is no such problem in the calculation of the joint moments  $\mu_{11}$  and  $\mu_{21}$  while  $3 < \alpha < 4$ . This is because the sign of  $\cos(\vec{k} \cdot \vec{R})$  alternates as  $k$  tend to infinity, so the integral over the short scales (large  $k$ ) is then equal to the sum of a decreasing series with an alternating sign.

We clearly do not expect Eq. (34) to hold at the long scales ( $k \rightarrow 0$ ), since there is finite energy in the spectrum. However, even if the spectrum did go to infinity at that limit, this would not pose a problem, since we require moments of the increment, which converge even in that case. Berry and Blackwell (1981) considered the mean square increment:

$$\Delta(\vec{R}) = \left\langle \left( \eta(\vec{x}) - \eta(\vec{x} + \vec{R}) \right)^2 \right\rangle. \quad (35)$$

We will require in addition the correlation between the height and the square of the height increment (or, equivalently, the correlation between the square of the height and the height increment), which we choose to call the BIAS moment, since it will be used later to calculate the sea state bias. It is defined by:

$$\begin{aligned} T(\vec{R}) &= \left\langle \eta(\vec{x}) \left( \eta(\vec{x}) - \eta(\vec{x} + \vec{R}) \right)^2 \right\rangle \\ &= \left\langle \eta(\vec{x})^2 \left( \eta(\vec{x}) - \eta(\vec{x} + \vec{R}) \right) \right\rangle. \end{aligned} \quad (36)$$

These functions can be related to the joint height moments (30,31):

$$\begin{aligned} \Delta(\vec{R}) &= 2(\mu_{20} - \mu_{11}) \\ &= 2 \iint d\vec{k} F(\vec{k})(1 - \cos(\vec{k} \cdot \vec{R})) + O(\epsilon^4) \end{aligned} \quad (37)$$

$$\begin{aligned} T(\vec{R}) &= \mu_{30} - \mu_{21} = \frac{1}{2} \iint d\vec{k}_1 \iint d\vec{k}_2 F(\vec{k}_1)F(\vec{k}_2) \\ &\times [(C_{12} - S_{12})(1 - \cos((\vec{k}_1 + \vec{k}_2) \cdot \vec{R})) \\ &+ (C_{12} + S_{12})(1 - \cos((\vec{k}_1 - \vec{k}_2) \cdot \vec{R})) \\ &+ 4C_{12}(1 - \cos(\vec{k}_1 \cdot \vec{R}))] + O(\epsilon^6) \end{aligned} \quad (38)$$

If the structure of the surface is self-affine over a range of scales which dominate the scattering of radiation with the radar wave length,  $\lambda$ , we may use dimensional analysis, to write:  $C, S \propto |\vec{k}_i|$  and  $F(\vec{k}_i) \propto |\vec{k}_i|^{-\alpha}$ . This implies that  $T(\gamma\vec{R}) = \gamma^{\{2\alpha-5\}}T(\vec{R})$ .

Thus, the theory of diffractals (Agnon and Stiassnie, 1991; Berry, 1979; Berry and Blackwell, 1981) can be applied using the form:

$$T(\vec{R}) \propto |\vec{R}|^{\{2\alpha-5\}} \quad (39)$$

We get for  $\vec{R} \rightarrow \vec{0}$ :

$$\begin{cases} \Delta(\vec{R}) &\rightarrow L^{2-D} R^D \\ T(\vec{R}) &\rightarrow M^{3-E} R^E \end{cases} \quad (40)$$

where  $R = |\vec{R}|$ , the topothesy<sup>1</sup> (Agnon and Stiassnie, 1991),  $L$ , and the BIAS topothesy,  $M$ , all have dimension of length (and are given in meters). The topothesy is defined by Berry to be the distance  $R = L$ , over which the mean square increment is  $\Delta(L) = L^2$ . It is typically a very small distance, since the characteristic slope of a segment between two points that are separated by a distance  $L$  is one radian. In analogy,  $M$  represents the Bias moment.  $D = D(\alpha) = \alpha - 2$  according to Berry, and  $E = E(\alpha) = 2\alpha - 5$  according to our above analysis<sup>2</sup>. We can modify the wave spectrum by introducing a high wavenumber cutoff to the spectrum,  $k_d$ , at scales smaller than some  $h$ . We may still retain, to a good approximation, the power law structure of  $T$ . However, the power  $E$  decreases and tends to  $\alpha - 2$ . While these limiting values can be deduced from the form of the equations, the intermediate range behavior is assessed by numerical calculations. The results of these computations will be discussed later.

Let us consider the correction to  $\Delta$  and  $T$  due to a drop in the spectrum  $F$ , for wave numbers smaller than the spectral peak,  $k_a$ . This introduces a term that is  $O((k_a R)^2)$  in both expressions. So, for  $4 \leq \alpha$  (which corresponds to a smooth, two dimensional sea surface) we will get, for  $\vec{R} \rightarrow \vec{0}$ :

$$\Delta(\vec{R}) \rightarrow B^2 R^2 \quad (41)$$

$$T(\vec{R}) \rightarrow M_s R^2 \quad (42)$$

$B^2$  is a mean square slope and  $M_s$  is a correlation between the height and the square of the slope along  $\vec{R}$ . Writing  $\vec{R} = (R, \phi)$ , we get

$$\begin{aligned} B^2 &= \cos^2 \phi \langle \eta_x^2 \rangle + 2 \cos \phi \sin \phi \langle \eta_x \eta_y \rangle + \sin^2 \phi \langle \eta_y^2 \rangle \\ M_s &= \cos^2 \phi \langle \eta \eta_x^2 \rangle + 2 \cos \phi \sin \phi \langle \eta \eta_x \eta_y \rangle + \sin^2 \phi \langle \eta \eta_y^2 \rangle \end{aligned}$$

where  $\eta_x$  and  $\eta_y$  are the slopes in the  $x$  and  $y$  directions. Both these quantities,  $B^2$  and  $M_s$ , appear in specular point reflection models. Thus, specular point reflection models may only be appropriate for power law models when  $4 \leq \alpha$  (smooth surfaces).

For  $R$  big enough the correlation between the two points approaches zero, and we will get for  $R \rightarrow \infty$ :

$$\begin{cases} \Delta(\vec{R}) \rightarrow 2H^2 \\ T(\vec{R}) \rightarrow \mu_{30} \end{cases} \quad (43)$$

A numerical investigation of an isotropic spectrum with  $\alpha = 3.5$ ,  $k_a = g/U^2$ ,  $U = 10$  m/sec and  $k_d = 2\pi/h$  with  $h = 0.4$  m, shows good agreement with the above analysis. In Fig. 2, we plot the variation of  $\ln(\Delta(\vec{R})/A)$  vs.  $\ln(R)$  (in Fig. 2a), and  $\ln(T(\vec{R})/A^2)$  vs.  $\ln(R)$  (in Fig. 2b). When  $Rk_d < 2\pi$  both  $D$  and  $E$  are about 2, while, when  $Rk_d > 1$  both increments reach

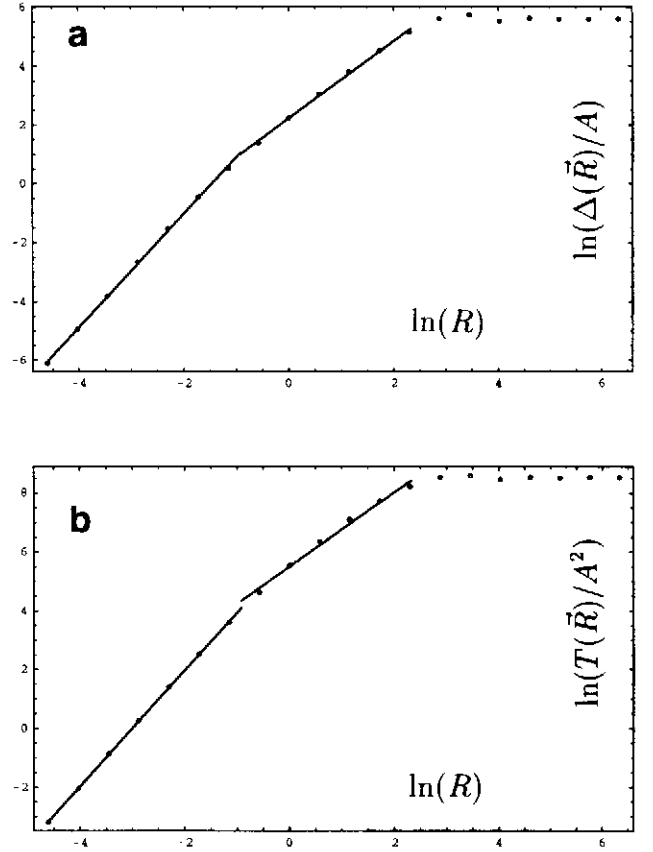


Fig. 2. The variation of (a)  $\ln(\Delta(\vec{R})/A)$  vs.  $\ln(R)$ , (b)  $\ln(T(\vec{R})/A^2)$  vs.  $\ln(R)$ . Both are calculated for isotropic spectrum,  $F(\vec{R}) = Ak^{-\alpha}$   $k_a \leq k \leq k_d$ , with the parameters:  $\alpha = 3.5$ ,  $k_a = g/U^2$   $m^{-1}$ ,  $k_d = 2\pi/h$   $m^{-1}$ ; where the wind speed at height 10m above sea level  $U = 10$  m/sec, and the lower cutoff  $h = 0.4$  m. To demonstrate the slopes in different regions we add best fit lines. The regions' boundaries were chosen to be  $Rk_d = 2\pi$  and  $Rk_a = 1$ , in both figures. In (a) the slopes are 1.93 for the shorter lengths of  $R$  and 1.31 in the intermediate region. In (b) the slopes are 1.97 for the shorter lengths of  $R$  and 1.25 in the intermediate region.

a plateau. The first limit can be shown by the approximation  $1 - \cos z \sim z^2/2$ , while the second is due to the fact that the oscillating integrands vanish. At the intermediate range,  $2\pi < Rk < 1$ ,  $D$  is approximately  $\alpha - 2 = 1.5$  and  $E$  is monotonic decreasing, with an average value of 1.5.

Similar results are obtained for  $\alpha = 4$ , and are plotted in Fig. 3.

### 3.2 Joint distribution function

Following the theory of Longuet-Higgins (1963), the joint distribution function  $P(\zeta_1, \zeta_2)$  which describes the probability for sea surface elevations  $\zeta_1$  and  $\zeta_2$  at the points

<sup>1</sup>  $L$  satisfies  $L^{4-\alpha} = \frac{4A}{\alpha-2} \frac{2^{2-\alpha} \Gamma(2-\alpha/2) \pi}{\Gamma(\alpha/2)}$

<sup>2</sup>  $D$  should not be confused with the fractal dimension of the sea surface, which is  $4 - \alpha/2$  for  $2 < \alpha < 4$  (Stiassnie et al., 1991)

$\vec{R}_1$  and  $\vec{R}_2$  respectively, is:

$$P(\zeta_1, \zeta_2) = \frac{1}{2\pi H^2 \sqrt{1-\rho^2}} \exp\left\{-\frac{f_1^2 - 2\rho f_1 f_2 + f_2^2}{2(1-\rho^2)}\right\} \times \left[1 + \frac{1}{6}(\lambda_{30} H_{30} + 3\lambda_{21} H_{21} + 3\lambda_{12} H_{12} + \lambda_{03} H_{03}) + O(\epsilon^2)\right] \quad (44)$$

where:

$$\lambda_{mn} = \mu_{mn}/H^{m+n} \quad m+n \leq 3 \quad (45)$$

$$\rho = \lambda_{11} \quad (46)$$

$$\zeta_i = H f_i \quad i = 1, 2 \quad (47)$$

$$H_{mn} = (-1)^{m+n} \exp\left\{\frac{f_1^2 - 2\rho f_1 f_2 + f_2^2}{2(1-\rho^2)}\right\} \times \frac{\partial^{m+n}}{\partial f_1^m \partial f_2^n} \exp\left\{-\frac{f_1^2 - 2\rho f_1 f_2 + f_2^2}{2(1-\rho^2)}\right\} \quad (48)$$

with the asymptotic order:

$$\lambda_{mn} = O(\epsilon^{m+n-2}) \quad (49)$$

therefore we get the joint distribution function as an asymptotic series.

In the above notation,  $\Delta(\vec{R}) = 2H^2(1-\rho)$  and  $T(\vec{R}) = H^3(\lambda_{30} - \lambda_{21}) = H^3(\lambda_{03} - \lambda_{12})$ .

#### 4 The intensity integral

In order to find the sea state bias which is the effect of the sea waves nonlinearity on the radar return waveform, we should calculate the intensity integral (Eq. 19) up to  $O(\epsilon)$ . Those calculations are quite complicated. In order to bring out the physics, we shall use some approximations.

The averaging will be done by using the joint probability distribution function  $P(\zeta_1, \zeta_2)$  (Eq. 44). By straightforward calculations (Gradshteyn and Ryzhik, 1965), assuming that  $1/(k_\lambda H) = O(\epsilon)$ , we get for the average in Eq. (19), see the Appendix for details:

$$\begin{aligned} \langle \dots \rangle = & \left(1 + \frac{16k_\lambda^2}{\sigma_1} T(\vec{R}) \left(\beta - \frac{R_1^2 + R_2^2}{2\sigma_1 z'}\right)\right) \times \\ & a_0^2 \frac{\sigma}{\sigma_1} \frac{1}{\sqrt{Q}} \exp\left\{-2k_\lambda^2 \Delta(\vec{R}) Q_1\right. \\ & - i \frac{k_\lambda}{z'} (R_1^2 - R_2^2) \left(\frac{4\Delta(\vec{R})}{\sigma_1^2}\right) Q_1 \\ & - 2\beta^2 Q_0 + 2\beta \left(\frac{R_1^2 + R_2^2}{\sigma_1 z'}\right) Q_0 \\ & - \left(\frac{R_1^4 + R_2^4}{\sigma_1^2 z'^2}\right) \left(\frac{\sigma^2 + 8H^2}{\sigma^2 Q}\right) \\ & \left. + \frac{16H^2}{\sigma^2 Q} \left(\frac{R_1 R_2}{\sigma_1 z'}\right)^2 \left(1 - \frac{\Delta(\vec{R})}{2H^2}\right)\right\} \quad (50) \end{aligned}$$

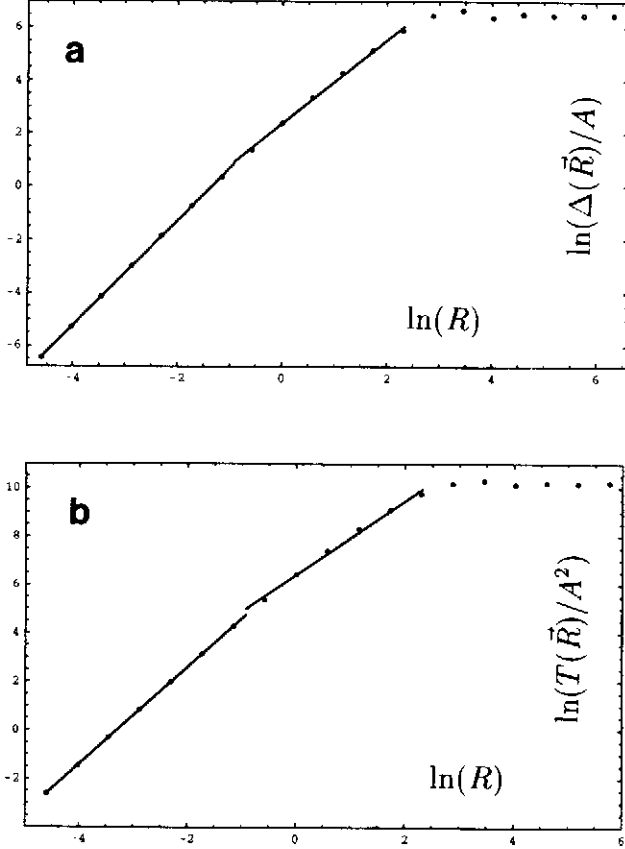


Fig. 3. The same as in Fig. 2, with  $\alpha = 4$ . The slopes in (a) are 1.97 and 1.58; The slopes in (b) are 2.00 and 1.54;

where  $\beta = c\tau/\sigma_1$  (a nondimensional variable) is the normalized time,  $\sqrt{\sigma_1 z'}$  is the radius of the illuminated sea area at which the intensity reaches its maximum. It depends on the sea state (wave height) and the radar pulse through the relation:  $\sigma_1^2 = \sigma^2 + 16H^2$ .

$Q$ ,  $Q_0$ ,  $Q_1$  are smooth bounded functions which tend to one as  $|\vec{R}| \rightarrow 0$ .  $Q = 1 + 64H^4/(\sigma_1^2 \sigma^2)(1 - \rho^2)$ ,  $Q_0 = (1 + \Delta(\vec{R})/\sigma^2)/Q$  and  $Q_1 = (1 - \Delta(\vec{R})/\sigma^2)/Q$ .

Putting the above into the intensity integrals and changing the coordinates as follows:  $\vec{R} = \vec{R}_1 - \vec{R}_2$ ,  $\vec{R}_0 = (\vec{R}_1 + \vec{R}_2)/2$  we get:

$$I = \left( \frac{k_\lambda a_0}{2\pi z^2} \right)^2 \frac{\sigma}{\sigma_1} \iint d\vec{R} \iint d\vec{R}_0 \frac{1}{\sqrt{Q}} \left( 1 - \frac{16k_\lambda^2}{\sigma_1} T(\vec{R})(y + \gamma) \right) * \exp \left\{ -2k_\lambda^2 \Delta(\vec{R}) Q_1 + i \frac{2k_\lambda}{z'} \vec{R} \cdot \vec{R}_0 Q_2 - 2Q_0(y + \gamma)^2 - \frac{2\sigma_1^2}{\sigma^2} \frac{\vec{R} \cdot \vec{R}_0}{\sigma_1 z'} Q_1 \right\} \quad (51)$$

where:  $y = R_0^2/\sigma_1 z'$ ,  $q' = R/\sqrt{\sigma_1 z'}$ ,  $\gamma = q'^2/4 - \beta$  and  $Q_2 = 1 - 4\Delta(\vec{R})Q_1/\sigma_1^2$ .

If we assume that the main contribution to the integrals is while  $|\vec{R}_1 - \vec{R}_2|$  is small because the correlation function decreases with distance, we will arrive at Berry and Blackwell's (1981) formula:

$$I = \left( \frac{k_\lambda a_0}{2\pi z^2} \right)^2 \frac{\sigma}{\sigma_1} \iint d\vec{R}_0 e^{-2(y-\beta)^2} \iint d\vec{R} \exp \left\{ -2k_\lambda^2 \Delta(\vec{R}) + i \frac{2k_\lambda}{z'} \vec{R} \cdot \vec{R}_0 \right\} \quad (52)$$

Rewriting (51) in polar coordinates  $\vec{R}_0 = (R_0, \theta)$ ,  $\vec{R} = (R, \phi)$ , gives:

$$I = \left( \frac{k_\lambda a_0}{2\pi z^2} \right)^2 \frac{\sigma z'}{2} \iint d\vec{R} \int_{-\pi}^{\pi} d\theta \int_0^\infty dy \frac{1}{\sqrt{Q}} \left( 1 - \frac{16k_\lambda^2}{\sigma_1} T(\vec{R})(y + \gamma) \right) * \exp \left\{ -2k_\lambda^2 \Delta(\vec{R}) Q_1 - i2pq' \sqrt{y} Q_2 \cos(\theta - \phi) - 2Q_0(y + \gamma)^2 - \frac{2\sigma_1^2}{\sigma^2} q'^2 y \cos^2(\theta - \phi) Q_1 \right\} \quad (53)$$

where  $p = k_\lambda \sigma_1 \gg 1$ . The term,  $-2Q_0(y + \gamma)^2$  in the exponent, ensures convergence of the integral.

In order to calculate those integrals we note that for  $\Delta(\vec{R}) = H^2 O(1)$  the integrands are exponentially small ( $e^{-2k_\lambda^2 \Delta(\vec{R})} = O(e^{-1/\epsilon^2})$ ). Therefore, the dominant interval will be  $R \in [0, \rho_0]$  where  $\Delta(\rho_0) = H^2$ . This will give us  $\rho_0 = H(H/L)^{(4-\alpha)/(\alpha-2)}$ , which is large since  $H \gg L$ . The variable  $q'$  is bounded in this interval by  $L(H/L)^{2/(\alpha-2)}/\sqrt{\sigma_1 z'} \approx 3 \cdot 10^{-3}$  for typical values of  $z$ ,  $H$ ,  $L$  and  $\alpha$ . Therefore, we assume  $q' = O(\epsilon^2)$  and  $\gamma = -\beta + O(\epsilon^4)$  in this interval. The exponential decreasing with  $y$  suggests  $y = O(1)$  as the dominant integration interval.

Some more straightforward calculations will bring us to the final estimate

$$I = \frac{a_0^2 \sigma z'}{8z^4} \left\{ \frac{1}{2} \sqrt{\frac{\pi}{2}} [1 + \Phi(\sqrt{2}\beta)] \sigma_F - e^{-2\beta^2} T_F \right\} \quad (54)$$

plus higher order terms, where  $\Phi(z) = \frac{2}{\pi} \int_0^z e^{-t^2} dt$  is the probability integral.  $\sigma_F$  is the Radar Cross Section,  $T_F$  is the nonlinearity effect on the intensity:

$$\sigma_F = \frac{2k_\lambda^2}{\pi} \iint d\vec{R} e^{-2k_\lambda^2 \Delta(\vec{R})} \quad (55)$$

$$T_F = \frac{8k_\lambda^4}{\pi \sigma_1} \iint d\vec{R} T(\vec{R}) e^{-2k_\lambda^2 \Delta(\vec{R})}. \quad (56)$$

The index  $F$  denotes the "fractal" model ( $\alpha < 4$ ), but the results are valid for other spectra as well.

Using the index  $s$  for smooth sea ( $4 \leq \alpha$ ), assuming isotropic sea (Eqs. 41, 42 with  $B^2 = \langle \eta_x^2 \rangle = \langle \eta_y^2 \rangle$ ,  $M_s = \langle \eta \eta_x^2 \rangle = \langle \eta \eta_y^2 \rangle$  and  $\langle \eta_x \eta_y \rangle = \langle \eta \eta_x \eta_y \rangle = 0$ ) we get

$$\left. \begin{aligned} \sigma_s &= 1/B^2 \\ T_s &= 2M_s/(\sigma_1 B^4) \end{aligned} \right\} \Rightarrow \frac{T_s}{\sigma_s} = \frac{2}{\sigma_1} \frac{M_s}{B^2} \quad (57)$$

Finally we write the intensity (54), due to the fact that the main contribution for the second part is for  $\beta = O(1)$ , as:

$$I = \frac{a_0^2 \sigma z'}{8z^4} \sqrt{\frac{\pi}{2}} \sigma_F \left\{ \frac{1}{2} [1 + \Phi(\sqrt{2}\beta)] - \sqrt{\frac{2}{\pi}} \frac{T_F}{\sigma_F} e^{-2\beta^2} \right\} \quad (58)$$

where the time  $\tau$  appears through  $\beta = c\tau/\sigma_1$ .

In real measurements the intensity tail (plateau region) decreases (e.g., Barrick and Lipa, 1985). We did not include this effect in our analysis, since our main goal is to model the leading edge of the return pulse. Thus the result is only good for  $|\beta| < 1$ , which is the interval of interest.

## 5 The sea state bias

In order to find the sea level height, the mid-time return point must be found. Following Srokosz (1987) we define the normalized intensity for further analysis:

$$\bar{I}(\tau) = I(\tau) / \left( \frac{a_0^2 \sigma z'}{8z^4} \sqrt{\frac{\pi}{2}} \sigma_F \right). \quad (59)$$

The estimation of the bias due to tracking the half-power point,  $\tau_{1/2}$ , is obtained by solving

$$\bar{I}(\tau_{1/2}) = \frac{1}{2}. \quad (60)$$

Noting that,  $\Phi(z) \sim 2z/\sqrt{\pi}$ ,  $e^{-z^2} \sim 1 - z^2$  as  $z \rightarrow 0$ , will lead us to the solution (Srokosz, 1987):

$$\beta_{1/2} = \frac{c\tau_{1/2}}{\sigma_1} = \frac{T_F}{\sigma_F} + O(\epsilon^2) \quad (61)$$



Note, that  $\tau_{1/2} \neq 0$  when  $T_F \neq 0$ .  $\tau_{1/2}$  is positive because of the nonlinearity of the sea surface.

Thus,  $\frac{1}{2}c\tau_{1/2}$  is the sea state bias,  $\eta_{em}$ , which describes the shift between the mean sea level and the level that corresponds to measuring half of the maximum intensity.

$$\eta_{em} = -\frac{\sigma_1 T_F}{2 \sigma_F} + \sigma_1 O(\epsilon^2) \quad (62)$$

where  $\sigma_1 = \sqrt{\sigma^2 + 16H^2}$ ,  $\sigma_F = \frac{2k_\lambda^2}{\pi} \iint d\vec{R} e^{-2k_\lambda^2 \Delta(\vec{R})}$ ,  $T_F = \frac{8k_\lambda^4}{\pi \sigma_1} \iint d\vec{R} T(\vec{R}) e^{-2k_\lambda^2 \Delta(\vec{R})}$ , and the moments:  $H^2 = \mu_{20}$ ,  $\Delta(\vec{R}) = 2(\mu_{20} - \mu_{11})$  and  $T(\vec{R}) = \mu_{30} - \mu_{21}$ .

In order to simplify the derivation, we assume an isotropic wave field. This is of course unrealistic (although the short wave field which has an important effect on the sea state bias may be nearly isotropic), still, we can expect to get the right trend.

In the case of isotropic smooth sea (57)

$$\eta_{em} = -\frac{\sigma_1 T_s}{2 \sigma_s} = -\frac{\langle \eta \eta_x^2 \rangle}{\langle \eta_x^2 \rangle} = -\frac{\langle \eta \eta_y^2 \rangle}{\langle \eta_y^2 \rangle} \quad (63)$$

( $-H\lambda_{120}$  and  $-H\lambda_{102}$  in Srokosz (1986) notations). (63) is the same as Srokosz (1986, Eq. (26)), for isotropic sea, since the cross-skewness parameter,  $\gamma$ , becomes  $\lambda_{120} + \lambda_{102}$  in this case.

However, our result differs from Srokosz (1987, Eq. 2). We did not get a term that is proportional to the skewness, but only the term that is proportional to the cross-skewness parameter,  $\gamma$ .

Using the "fractal" model for the joint moments,  $\Delta(\vec{R}) = L^{2-D} R^D$ ,  $T(\vec{R}) = M^{3-E} R^E$  i.e. a power law spectrum, we obtain:

$$\begin{aligned} \sigma_F &= \frac{2k_\lambda^2}{\pi} 2\pi \int_0^\infty e^{-\{2k_\lambda^2 L^{2-D} R^D\}} R dR \\ &= \frac{4}{D} (2k_\lambda^{2-D} L^{2-D})^{-2/D} \Gamma\left(\frac{2}{D}\right) \\ T_F &= \frac{8k_\lambda^4}{\pi \sigma_1} 2\pi \int_0^\infty M^{3-E} R^E e^{-2k_\lambda^2 L^{2-D} R^D} R dR \\ &= \frac{16}{D k_\lambda \sigma_1} (k_\lambda M)^{3-E} (2k_\lambda^{2-D} L^{2-D})^{-\frac{2+E}{D}} \Gamma\left(\frac{2+E}{D}\right) \\ \eta_{em} &= -\frac{\sigma_1 T_F}{2 \sigma_F} = -\frac{2}{k_\lambda} (k_\lambda M)^{3-E} \\ &\quad (2k_\lambda^{2-D} L^{2-D})^{-\frac{E}{D}} \frac{\Gamma((2+E)/D)}{\Gamma(2/D)} \end{aligned} \quad (64)$$

We see a dependence of the sea state bias on the radar wavenumber  $k_\lambda$ ,  $\eta_{em} \propto k_\lambda^{2(D-E)/D}$ . Thus, our model exhibits dependence of the sea state bias on the radar frequency. This feature is known from field experiments of Walsh et al. (1989, 1991), but not captured by the specular point reflection model. Also, we see nonlinear dependence on  $H_{1/3}$ ,  $\eta_{em} \propto H_{1/3}^{2+2(D-E)/D}$ , since  $A \propto H_{1/3}^2$ .

A	$H_{1/3}$	$\sigma_F$	$T_F$	$\eta_{em}$	$\frac{\eta_{em}}{H_{1/3}}$	$\frac{\eta_{em}}{A}$
.0005	1.04	90.6	.535	-.00937	.898	18.7
.001	1.48	45.1	.506	-.0188	1.27	18.8
.002	2.09	22.4	.457	-.0372	1.78	18.6
.003	2.56	14.9	.419	-.0553	2.16	18.4
.005	3.30	8.96	.366	-.0910	2.76	18.2
.008	4.18	5.62	.316	-.145	3.46	18.1
.01	4.67	4.51	.293	-.180	3.86	18.0

**Table 1.** Relying on the form of  $\Delta(\vec{R})/A$  and  $T(\vec{R})/A^2$  calculated in Fig. 2, we change the parameter  $A$  (given in  $\sqrt{m}$ , where  $m$  is the length given in meters) and calculate the different parameters. The forms are given for a spectrum with:  $\alpha = 3.5$ ,  $k_a = g/U^2 \text{ m}^{-1}$ ,  $k_d = 2\pi/h \text{ m}^{-1}$ ; where the wind speed at height 10m above sea level  $U = 10 \text{ m/sec}$ , and the lower cutoff  $h = 0.4 \text{ m}$ . For different values of the spectrum coefficient  $A$  we calculate: the significant wave height  $H_{1/3}$  (m),  $\sigma_F$ ,  $T_F$ , the sea state bias  $\eta_{em}$  for radar wave length 3cm and its relation to the significant wave height  $\eta_{em}/H_{1/3}$  in percentage, and its relation to the spectrum coefficient  $A$ .

## 6 Numerical Results

In order to get a general idea of the variation of the sea state bias as a function of the wave spectrum's parameters, we carried out calculations for a simple model of the wave spectrum (34), with  $\alpha = 3.5$  and 4.0. We take the form for  $\Delta(\vec{R})$  and  $T(\vec{R})$ , as calculated for the spectrum with  $k_a = g/U^2$  and  $k_d = 2\pi/h$  (see Figures 2 and 3), for different values of the parameter  $A$ . The radar wavelength was chosen to be  $0.03 \text{ m}$  (10 GHz). Calculating the sea state bias (62), after using (55, 56), we get the results summarized in Table 1. For different wave heights we see that the sea state bias variation is proportional to the parameter  $A$  of the wave spectrum. This was expected, since the cutoff suggests that the sea is smooth for short waves. Thus, both  $D$  and  $E$  can be approximated as 2 for the relevant scales.

When we will push  $h$  to zero, we will get the "fractal" presentation, where  $D = \alpha - 2$  and  $E = 2\alpha - 5$ . Thus, for  $\alpha = 3.5$ ,  $\eta_{em} \propto k_\lambda^{-2/3}$  and  $\eta_{em} \propto A^{2/3}$ .

To summarize the results, we compare Equations (1) and (64). We recall that Eq. (1) ignores the nonlinear dependence of the electromagnetic bias on the wave height, leading to a spread of the results.

In Fig. 4 we plot the percentage of the sea state bias of the significant wave height,  $|\eta_{em}/H_{1/3}| \%$ , as a func-

A	$H_{1/3}$	$\sigma_F$	$T_F$	$\eta_{em}$	$\frac{\eta_{em}}{H_{1/3}}$	$\frac{\eta_{em}}{A}$
.0005	1.62	126	1.70	-.0229	1.42	45.8
.001	2.29	62.9	1.52	-.0456	2.00	45.6
.002	3.23	31.4	1.29	-.0909	2.81	45.5
.003	3.96	20.9	1.15	-.136	3.44	45.5
.005	5.11	12.5	.961	-.227	4.44	45.4
.008	6.46	7.84	.798	-.363	5.61	45.4
.01	7.23	6.27	.727	-.453	6.27	45.3

**Table 2.** The same as in Table 1 but, relying on the form of  $\Delta(\vec{R})/A$  and  $T(\vec{R})/A^2$  calculated in Fig. 3, with  $\alpha = 4.0$ .

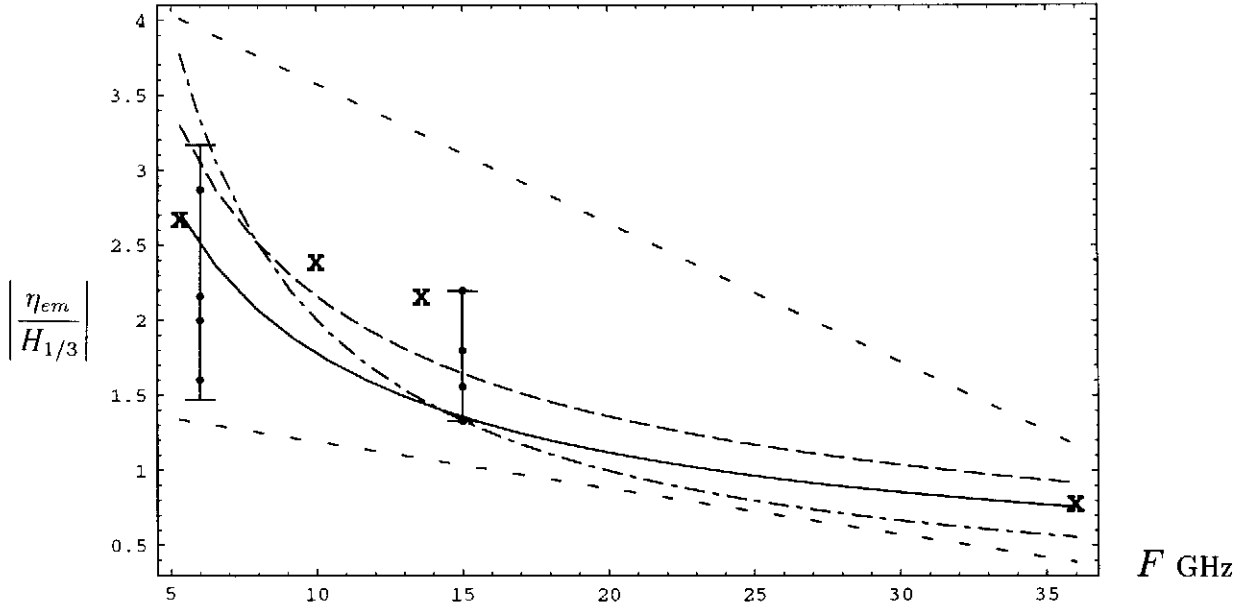


**Fig. 4.** Results of the comparison between Equations (1) and (64). The percentage of the sea state bias of the significant wave height,  $|\eta_{em}/H_{1/3}|%$ , as a function of the radar frequency,  $F$ , in GHz.

The two dashed lines (---) present the lower and upper bounds of Eq. (1); The four Xs, at  $F = 5.3, 10, 13.6, 36$ , are the radar frequencies used in Walsh's experiments (Walsh et al., 1989, 1991). The curved lines present our estimation according to Eq. (64) and the results obtained in the tables.

The full line (—)  $\alpha = 3.5$ ,  $A = 0.002$ ,  $H_{1/3} = 2.09$ .

The dashed line (---)  $\alpha = 3.5$ ,  $A = 0.003$ ,  $H_{1/3} = 2.56$ .

The dash-dotted line (-.-.-)  $\alpha = 4.0$ ,  $A = 0.001$ ,  $H_{1/3} = 2.29$ .

The two vertical segments, at  $F = 6, 15$ , are taken from Rodriguez et al. (1992) Fig. 9a. The four dots on each line were given for four different significant wave height (2.5, 1.5, 0.87, 0.38 meters).

tion of the radar frequency,  $F$ , in GHz. We have shown the lower and upper bounds of Eq. (1) and the mean experimental values associated with it. The results obtained by Eq. (64) and the results obtained in the tables, are seen to fall within those bounds. Both values used,  $\alpha = 3.5$  and  $\alpha = 4.0$ , provide good agreement, still the trend of the  $\alpha = 3.5$  curves is closer to Eq. (1). We also show computational results of Rodriguez et al. (1992). These results also fall in the same range.

## 7 Conclusions

An alternative model was proposed for the study of the sea state bias in radar altimetry. This model is based on the Kirchhoff approximation and is more general than the specular point reflection model which has been widely used. The present model does not assume that the surface is smooth, and addresses roughness on small scales. The cutoff in the spectrum was introduced to describe the actual water wave spectrum, and not in order to make the scattering integral converge. The statistical moments of the free surface relate heights and increments at two points. For spectra that are not "smooth", the bias was found to vary with the radar frequency.

## Appendix A Derivation of Eq. (50)

The average in Eq. (19) is calculated by using the joint probability distribution function  $P(\zeta_1, \zeta_2)$  (44).

$$\begin{aligned} & \left\langle a(T_1)a(T_2)e^{-2ik_\lambda(\eta(\vec{R}_1)-\eta(\vec{R}_2))} \right\rangle = \\ & K \iint \exp\{-p(f_1^2 + f_2^2) + 2(q_1 f_1 + q_2 f_2 + q_3 f_1 f_2)\} \\ & \times [1 + L(f_1^3 + f_2^3) + M f_1 f_2 (f_1 + f_2) + N(f_1 + f_2)] df_1 df_2 \quad (A1) \end{aligned}$$

The constants in the above Eq. (A1) are:

$$K = \frac{1}{2\pi H^2 \sqrt{1-\rho^2}} \quad (A2)$$

$$L = \frac{-\lambda_{30}(1+\rho+\rho^2) + 3\lambda_{21}}{6(1-\rho^2)^2(1+\rho)} \quad (A3)$$

$$M = \frac{3\rho\lambda_{30} - \lambda_{21}(1-\rho+\rho^2)}{6(1-\rho^2)^2(1+\rho)} \quad (A4)$$

$$N = \frac{3\lambda_{30} + \lambda_{21}(1-2\rho)}{6(1-\rho^2)(1+\rho)} \quad (A5)$$

$$p = \frac{4H^2}{\sigma^2} + \frac{1}{2(1-\rho^2)} \quad (A6)$$

$$q_1 = -\frac{2Hc}{\sigma^2}(\tau - \frac{R_1^2}{cz'}) - ik_\lambda H \quad (A7)$$

$$q_2 = -\frac{2Hc}{\sigma^2}(\tau - \frac{R_2^2}{cz'}) + ik_\lambda H \quad (A8)$$

$$q_3 = \frac{\rho}{2(1 - \rho^2)} \quad (A9)$$

Straightforward calculations, and then collecting the higher order terms with  $(ik_\lambda H)^2$  gives us Eq. (50).

**Acknowledgements.** This research was supported by the Fund for Promotion of Research at the Technion. We thank Prof. M. Stiassnie for useful discussions and the reviewers for their helpful comments.

## References

- Y. Agnon & M. Stiassnie, Remote sensing of roughness of fractal sea surface, *Journal of Geophysical Research* **96** (C7) (1991) 12773-12779.
- D.E. Bar, Diffraction from a fractal sea surface, *M.Sc. Thesis* (1992) Technion, Haifa.
- D.E. Barrick & B.L. Lipa, Analysis and interpretation of altimeter sea echo, *Adv. in Geophysics* **27** (1985) 61-100.
- M.V. Berry, On deducing the form of surfaces from their diffracted echoes, *J. Phys. A: Gen. Phys.* **5** (1972) 272-291.
- M.V. Berry, Diffractals, *J. Phys. A: Gen. Phys.* **12** (1979) 781-797.
- M.V. Berry & T.M. Blackwell, Diffractals echoes, *J. Phys. A: Math. Gen.* **14** (1981) 3101-3110.
- G.H. Born & M.A. Richards, An empirical determination of the effects of sea state bias on SEASAT altimetry, *Journal of Geophysical Research* **87** C5 (1982) 3221-3226.
- R.E. Glazman, Near-nadir radar backscatter from a well developed sea, *Radio Sci.* **25** (1990) 1211-1219.
- R.E. Glazman, Surface gravity waves at equilibrium with a steady wind, *Journal of Geophysical Research* **99** C3 (1994) 5249-5262.
- R.E. Glazman, A. Fabrikant & M.A. Srokosz, Numerical analysis of the sea state bias for satellite altimetry, *Journal of Geophysical Research* **101** (C2) (1996) 3789-3799.
- R.E. Glazman, A. Greysukh & V. Zlotnicki, Evaluating models of sea state bias in satellite altimetry, *Journal of Geophysical Research* **99**, (C6) (1994) 12581-12591.
- R.E. Glazman & M.A. Srokosz, Equilibrium wave spectrum and sea state bias in satellite altimetry, *Journal of Physical Oceanography* **21** (1991) 1609-1621.
- R.E. Glazman & P.B. Weichman, Statistical geometry of a small surface patch in a developed sea, *Journal of Geophysical Research* **94** (C4) (1989) 4998-5010.
- J.S. Gradshteyn & I.M. Ryzhik, Table of integrals series and products (1965).
- M.S. Longuet-Higgins, The effect of non linearities on statistical distributions in the theory of sea waves, *J. Fluid Mech.* **17** (1963) 459-480.
- O.M. Phillips, Spectral and statistical properties of the equilibrium range in wind-generated gravity waves, *J. Fluid Mech.* **156** (1985) 505-531.
- E. Rodriguez, Y. Kim & J.M. Martin, The effect of small wave modulation on the Electromagnetic bias, *Journal of Geophysical Research* **97**, (C2) (1992) 2379-2389.
- M.A. Srokosz, On the joint distribution of surface elevation and slopes for a nonlinear random sea, with an application to radar altimetry, *Journal of Geophysical Research* **91** (C1) (1986) 995-1006.
- M.A. Srokosz, Reply, *Journal of Geophysical Research* **92** (C3) (1987) 2989-2990.
- M. Stiassnie, The fractal dimensions of the ocean surface, *Non-linear topics in ocean physics. Proc. Int. Sch. of Phys, Enrico Fermi* (1988).
- M. Stiassnie, Y. Agnon & L. Shemer, Fractal dimensions of random water surfaces, *Physica D* **47** (1991) 341-352.
- E.J. Walsh, F.C. Jackson, E.A. Uliana & R.N. Swift, Observations on electromagnetic bias in radar altimeter sea surface measurements, *Journal of Geophysical Research* **94**, (C10) (1989) 14575-14584.
- E.J. Walsh et al. Frequency dependence of electromagnetic bias in radar altimeter sea surface range measurements, *Journal of Geophysical Research* **96**, (C11) (1991) 20571-20583.
- O.I. Yordanov & O. Stoyanov, Detailed application of the Kirchhoff approximation to scattering by fractal-like rough surfaces, *Proc. URSI* **89** (1989) 512-514.